

Research article

Hygroscopic elongation of moisture-responsive polyamide 6 fibers copolymerized with polyetherdiamine and adipic acid

Wei-Hsiang Lin¹, Chang-Mou Wu^{1*}, Shamik Chaudhuri^{1,2}, Ta-Chung An³,
Po-Hsun Huang³

¹Department of Materials Science and Engineering, National Taiwan University of Science and Technology, 10607 Taipei, Taiwan (ROC)

²Department of Polymer and Process Engineering, Indian Institute of Technology Roorkee (IITR), Saharanpur Campus, 247001 Saharanpur,, Uttar Pradesh, India

³Taiwan Textile Research Institute, 23674 New Taipei City, Taiwan (ROC)

Received 3 November 2023; accepted in revised form 25 January 2024

Abstract. Smart materials represent an emerging and highly exploited category, particularly in the creation of textiles that can sense and respond to various external stimuli, such as temperature or humidity. This study introduces for the first time the hygroscopic elongation and drying shrinkage properties of stimulus-responsive single-component polyamide (PA) fibers copolymerized with polyetherdiamine and diethylenetriamine (DETA). PA copolymers containing 5–15% polyetherdiamine were comprehensively characterized, including nuclear magnetic resonance spectroscopy (NMR), Fourier transform infrared spectroscopy (FT-IR), relative viscosity, and differential scanning calorimetry (DSC) analyses. Subsequently, these PA copolymers were successfully melt-spun into fibers and knitted into double-layered fabrics. PA fibers containing 15% polyetherdiamine showed significant results, with a moisture-absorbing elongation of 15.6% and a drying shrinkage of 94.9%. The Q_{\max} and moisture regain of the PA fabric are $0.206 \text{ W} \cdot \text{cm}^{-2}$ and 4.4%, respectively. These moisture-driven, fiber-based smart textiles exhibit changes in breathability and shape retention at different humidity levels, thereby maintaining a more comfortable microclimate. Such textiles have great potential for widespread use in clothing, helping to improve comfort and adaptability.

Keywords: fibrous polymers, functional polymers, smart polymers, polymer chemistry, thermoplastic blends, hygroscopic elongation

1. Introduction

Stimuli-responsive materials exhibit visible physical, chemical, or biological changes when exposed to external stimuli. They can respond to stimuli in many ways, including structural change, color change, optical response, electrical response, thermal response, or chemical response. These responses can be harnessed to provide special functions for application in smart materials, reshaping materials, sensors, medical materials, energy storage devices, optoelectronic materials, etc.

Smart materials are representative of stimuli-responsive materials as they can recognize and respond to external stimuli to control the shape, color, chemical activity, and other characteristics of objects. They have been used in a wide range of applications, including robotics, automobile manufacturing, aerodynamics, construction materials, medical equipment, and textiles [1, 2].

Stimuli-responsive textiles represent a new class of textile materials that utilize elastic response properties upon exposure to external stimuli to provide

R1
R2
R3
R4
R5
R6
R7
R8
R9
R10
R11

*Corresponding author, e-mail: cmwu@mail.ntust.edu.tw
© BME-PT

their stimulus-response, which can eventually be utilized for human body comfort [3]. Such materials are typically produced by adding fiber-mixed products exhibiting full spectrum light, fluorescence, thermal effects, and so on. Full spectrum light and fluorescence effects, respectively, emit several brilliant colors under different light conditions, whereas thermal effects allow fibers to warm or chill the material when stimulated. A combination of these properties can stimulate the senses and create an amazing and interactive environment. For example, stimuli-responsive textiles could be used to create emotion recognition devices that enable people to better understand their own and others' emotions. Such textiles could also be used to create innovative and personalized products including sportswear, outdoor equipment, public transport seats, and mattresses.

When the temperature of the environment is lower than that of the human body, clothing fabrics should help keeping the body warm using a compact structure to prevent the transmission of body-generated heat. Moreover, the air entrapped within the small pores of this structure is heated by the body, further helping to maintain body temperature. In contrast, when the temperature of the environment is higher than that of the human body or during strenuous physical activities such as sports or exercise, the human body experiences sensible perspiration, which occurs at a much higher rate than insensible perspiration. A high rate of sensible perspiration moistens the skin in the form of sweat rather than evaporating, resulting in a sticky, uncomfortable feeling where the fabric surface contacts the skin. Therefore, body-comforting textiles should transport excessive heat and moisture in the form of both sensible and insensible perspiration from the human body to the surrounding environment, thereby helping to regulate the thermal and moisture balance within the body's microclimate [4–7].

Microencapsulated phase-change materials, shape-memory polymers, and low-critical-solution-temperature materials are among the most popular thermally responsive textiles developed for hot climates [8, 9]; these are typically fabricated using post-processing or thin-film methods. Notably, stimuli-responsive textiles with hygroscopic fibers can absorb sweat, elongate, and eventually swell, enlarging the pores within the fabric. This allows for the rapid evaporation of perspiration, thereby preventing sweat accumulation. Such smart textiles can repeatedly change

their structure from swollen to compact and vice versa according to changes in climatic and body conditions through this moisture regulatory function. Furthermore, researchers have reported that when two materials with different moisture absorption rates are spun side by side, the composite fiber elongates and reduces its curl when absorbing moisture, allowing the fabric pores to become even larger and further improve air permeability [10, 11].

Thus, the investigation of moisture-driven smart textiles is an active subject of emerging research in the worldwide textile sector. Jia *et al.* [12] demonstrated humidity-regulated torsional and tensile actuation of thermally twisted, coiled, and piled silk fibers and found that the actuation of textiles weaved from these fibers originated from the water absorption-induced loss of H-bonds within the silk protein and associated structural changes. Later, Guan *et al.* [13] fabricated a cotton fabric coated with a hydrophobic reduced graphene oxide inner layer and hydrophilic graphene oxide outer layer to realize a smart Janus textile with a wettability gradient structure and excellent liquid moisture transport performance. Noman *et al.* [14] investigated the roles of ZnO nanoparticle coatings on the thermo-physiological properties of cotton and polyester woven fabrics. In the authors' previous study, a poly (NIPAAm-co-HEMA-co-NMA) coating was applied to a polyester fabric to realize thermal responsiveness and moisture management in smart textile applications [15]. However, functionalized polyamide (PA)-based smart textiles with moisture-responsive properties have not been reported to date. In particular, single-component polyamide 6 (PA6) fibers, which are readily recyclable considering current environmental protection trends, can exhibit hygroscopic elongation and dry recovery properties.

Various methods have been developed to overcome the limitations associated with inadequate moisture absorption and improve wettability. Copolymerization modification or blending is generally applied throughout the industry owing to its consistent successful execution. In recent years, considerable effort has been dedicated to exploring copolymerization modifications by adding different chain extenders to solve the crucial application-based problems of PA6. Zhang *et al.* [16] proposed polymerization routes for the preparation of PA6-based polymers using different molar ratios of adipic acid, terephthalic acid, and other dibasic acid-blocking agents. The resulting

PA6-based polymers exhibited excellent mechanical and moisture absorption properties. Cousin *et al.* [17] prepared biobased PA copolymers by incorporating 2,5-furandicarboxylic acid during the hydrolysis reaction of caprolactam. The hygroscopicity of the resulting copolymers increased with increasing 2,5-furandicarboxylic acid concentration, whereas their glass transition temperature (T_g) decreased. Furthermore, the thermal stability and T_g of PA copolymers prepared by anionic polymerization were significantly improved by the addition of an aromatic chain extender, ethyl 4-aminobenzoate [18]. Indeed, incorporating 17 mol% of aromatic chain extender raised the T_g of a PA copolymer from 40 to 79 °C. Semi-aromatic component-modified PA6 was developed using caprolactam as the solvent for purified terephthalic acid and 1,6-hexanediamine; it exhibited excellent transparency and a high decomposition temperature [19].

Polyetheramines with polyethylene glycol (PEG) backbones have been widely explored as extensive functionalizing materials. Dutkiewicz and Boryniec [20] used polyetheramines as elasticizing chemical modifiers for caprolactam/lauryl lactam copolymers. Flexible polyether segments, such as polyoxypropylenetriamine, have been introduced into the PA chain to increase the impact resistance of carbon-fiber reinforced PA composites; these composites were coated with Jeffamine (a PEG backbone) and isocyanate to improve their mechanical and physical properties [21]. Rossi *et al.* [22] incorporated polyetheramines into Nylon 6,6 to enhance its wettability and antibacterial properties against *Staphylococcus aureus* and *Klebsiella pneumoniae*. In the present study, neat PA6 was reacted with polyetherdiamine to enhance its mechanical and moisture absorption properties, while diacid (adipic acid, AA) acted as a precursor for nylon production. Another critical aspect of such modifications is cross-linking. Diethylenetriamine (DETA) is a widely used curing and cross-linking agent in epoxy resins [23, 24]; however, researchers have also extensively applied this material to other polymers, including PA [25–28].

This study accordingly copolymerized neat PA6 with RE-900 and AA using a minute quantity of DETA as a cross-linker to enhance the resilience between molecular chains. This reaction was performed using a solid-state approach. The obtained PA6 copolymers were characterized using nuclear magnetic resonance

(^1H NMR) and Fourier-transform infrared (FT-IR) spectroscopy to verify their composition. Furthermore, the viscosities of the PA6-based copolymers were measured to determine their spinnability, and their thermal properties were determined using differential scanning calorimetry (DSC). Subsequently, PA6 fibers were melt-spun to evaluate the mechanical properties of yarns manufactured therefrom. Finally, the moisture absorption and regain of PA6 yarns and the fabrics woven from them were evaluated using gravimetric analysis to determine their ability to provide stimulus-response.

2. Experimental section

2.1. Materials

The caprolactam ($\geq 99\%$) used to produce PA6 was purchased from the China Petrochemical Development Corporation, Taipei, Taiwan. The RE-900 polyetherdiamine ($\geq 99\%$) was provided by the Huntsman Corporation, Texas, United States. The AA ($\geq 99\%$) was purchased from Ascend Performance Materials, Houston, Texas, United States. Finally, the DETA ($\geq 99\%$) was purchased from Sigma-Aldrich, St. Louis, Missouri, United States.

2.2. Polymer synthesis

The moisture-responsive copolymer was synthesized through the copolymerization modification of caprolactam, RE-900, AA, and DETA, as shown in Figure 1. Copolymers containing 0, 5, 10, and 15 wt% of RE-900 were denoted as neat PA6, PA6-5, PA6-10, and PA6-15, respectively; their properties are reported in Table 1. The caprolactam, RE-900, AA, and DETA were weighed at room temperature in quantities according to their desired molar ratios and placed in a reaction tank. The temperature was increased to 220 °C, and the tank was purged with nitrogen at 0.2 MPa pressure. Hydrolysis was subsequently performed in a nitrogen atmosphere for 120 min. The water circulation for condensation was stopped once the hydrolysis reaction was complete. Eventually, the pressure was released, and the water was discharged. When the reactor achieved normal pressure, the temperature was raised to 260 °C, and a vacuum environment was slowly applied, decreasing the pressure to 26664.5 Pa. Simultaneously, the torque condition of the rotating motor was observed to obtain pellets upon achieving the optimum conditions.

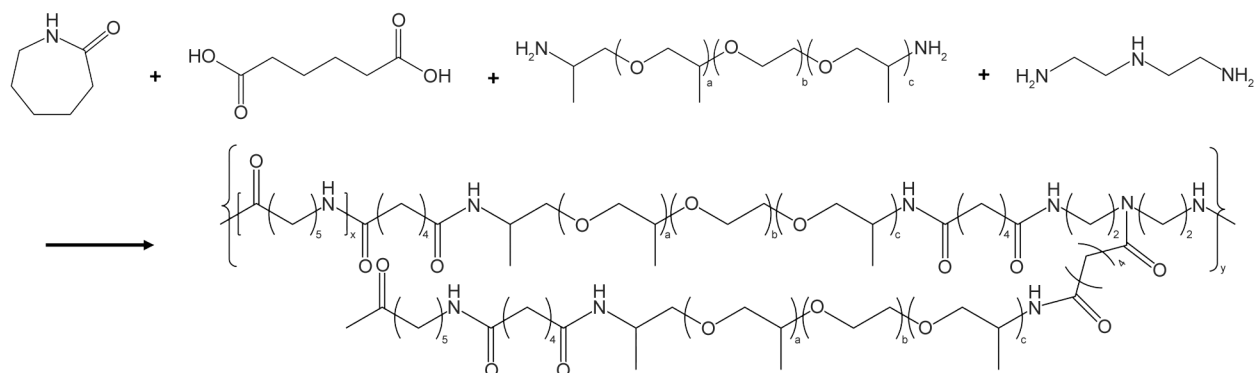


Figure 1. Schematic diagram of PA6 copolymerization reaction.

Table 1. PA6 copolymers with different RE-900 contents and their relative viscosities.

Sample	RE-900 [wt%]	DETA [mol%]	<i>RV</i> [–]	NH ₂ group
PA6	0	0.2	2.36	44
PA6-5	5	0.2	1.85	39
PA6-10	10	0.2	1.56	48
PA6-15	15	0.2	1.43	72

As shown in Table 1, as the RE-900 content increased, the relative viscosity (*RV*) of the PA6 decreased but remained within the spinnable range.

2.3. Fabrication of fiber specimen

The fibers were fabricated using an extruder with heating zones of 275, 285, 290, and 295 °C; the box temperature was 295 °C. The output pressure of the extruder was approximately 90 bar. The partially oriented yarn (POY) arrangement was 90 d/48 f (denier per filament); The Godet Rolls- GR1 and GR2 were 4250 and 4300 m/min, respectively, at room temperature; the Winder Roll (WR) was 4200 m/min. Finally, draw textured yarn (DTY) was created from the POY using a 70 d/48 f arrangement with a draw ratio of 1.2 and a speed of 500 m/min. These DTYs are then used to manufacture different types of single jersey fabrics using knitting machines. However, double-layer lattice knitted fabric was further considered for PA6-10 samples as it exhibited excellent yield, moisture regain, and drying shrinkage properties.

2.4. Characterization

The ¹H NMR spectra of PA copolymers were acquired using a JNM-ECZS 400 MHz spectrometer, JEOL Ltd., Tokyo, Japan, with trifluoroacetic acid-d as the solvent. Chemical shifts were reported as δ values in parts per million, referencing tetramethyl silane as an internal standard.

The FT-IR spectra of PA copolymers were recorded on a Nicolet iS50 ATR, Thermo Scientific, Massachusetts, United States. All FTIR measurements were conducted within the wavenumber range of 4000–400 cm⁻¹ using 32 accumulated scans at a resolution of 4 cm⁻¹. The relative viscosity (*RV*) of each PA copolymer was measured with a CT-1650 instrument from Schott (Mainz, Germany).

The viscosity was determined by grinding the corresponding pellets into a powder, which was then dried at 75 °C for one hour. After cooling to room temperature, 0.25 g of each powder was mixed with 25 ml of 96% concentrated sulfuric acid. This mixture was shaken at 50 °C for 40 min to completely dissolve the powder. The mixed solution was then placed in a water bath at 25 °C for 20 min. Finally, the *RV* of the solution was measured using a Schott/CT-1650 automatic viscometer, with the reported value for each PA representing the average of three measurements.

The melting point, crystallization temperature, heating enthalpy, and cooling enthalpy were determined using a differential scanning calorimeter (DSC25, TA Instruments, Delaware, United States). The samples underwent heating from 30 to 300 °C at a rate of 10 °C/min.

Surface textures and morphologies of the fabric samples were observed using a three-dimensional microscope (VHX-7000, Keyence, Osaka, Japan). The *Q*_{max} test (KES-F7 Thermo Labo II, Kyoto, Japan) was used to evaluate the cool feeling of textiles at 20±2 °C and 65±4%RH. Fabric samples measuring 20×20 cm were sandwiched between hot and cold plates at temperatures of 35±0.1 and 25±0.1 °C, respectively. The data obtained is the average of 5 samples.

The tensile properties of the DTYs were measured using a universal testing machine Comotech QC-508M2 (Comotech, Taichung, Taiwan), with a

crosshead speed of 200 mm/min. A minimum of five samples were tested for each PA to estimate the average value.

The DTY fiber was initially wound to a length of 50 cm using a winding machine. Subsequently, it underwent a boiling water treatment for 30 min and was then air-dried for 24 h. The initial length (L_1) of the soaked fiber was measured, followed by a second soaking in 25 °C water for 30 min. After removal from water, the final length (L_2) was measured, allowing for the calculation of moisture-absorbing elongation (ϵ) using the Equation (1):

$$\epsilon = \frac{L_2 - L_1}{L_1} \cdot 100\% \quad (1)$$

Moisture regaining tests were conducted by initially weighing 20 g of DTYs after drying at 105 °C for 2 h (W_1). Subsequently, the DTYs were reweighed after exposure to a 20 °C, 65%RH environment for 8 h (W_2). The moisture absorption (MA) was determined using the Equation (2):

$$MA(20^\circ\text{C}, 65\%RH) = \frac{W_2 - W_1}{W_1} \cdot 100\% \quad (2)$$

Further tests involved placing the DTYs in a 30 °C, 90%RH environment for 8 h and measuring the weight (W_3) (Equations (3) and (4)):

$$MA(30^\circ\text{C}, 90\%RH) = \frac{W_3 - W_1}{W_1} \cdot 100\% \quad (3)$$

$$\begin{aligned} \text{Moisture regains} &= \\ &= MA(30^\circ\text{C}, 90\%RH) - MA(20^\circ\text{C}, 65\%RH) \end{aligned} \quad (4)$$

The synthesis process of the PA copolymer, fiber and fabric fabrication, and all characterizations are illustrated in Figure 2.

3. Results and discussion

3.1. NMR spectroscopy

The ^1H NMR spectra with proton peaks for the PA6-5, PA6-10, and PA6-15 moisture-responsive copolymers are shown in Figure 3. All the major peaks of

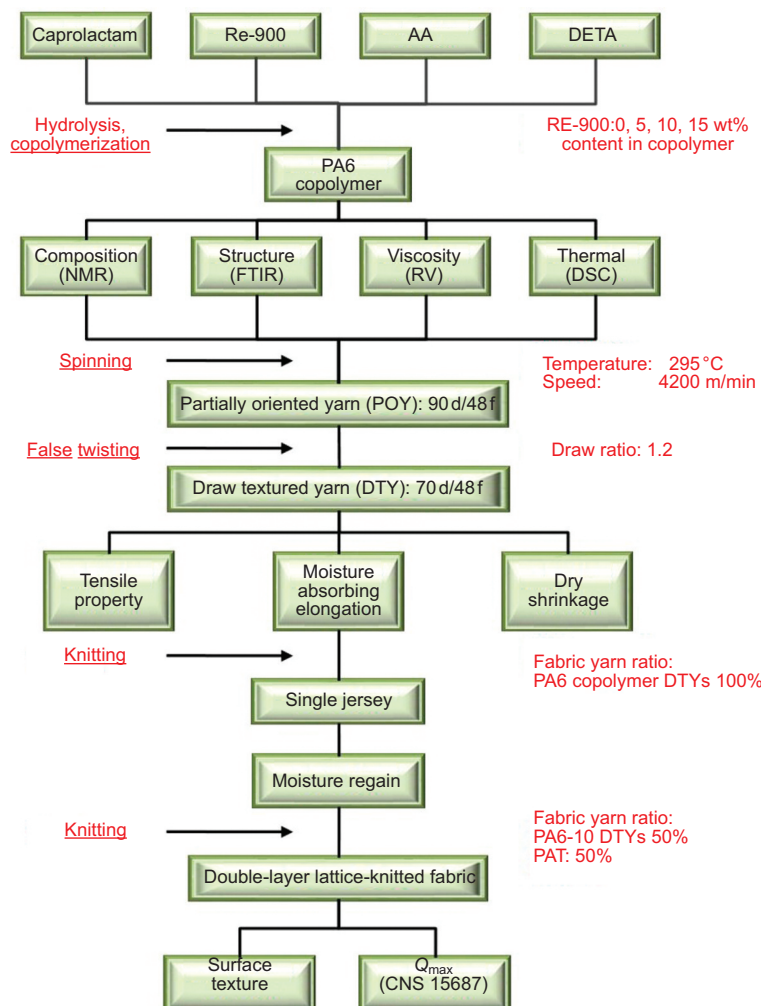


Figure 2. Illustration of the fabrication and characterizations of the PA6 copolymers and fibers.

the copolymers are between 1–4 and 12 ppm. The peaks at 11.5 ppm are attributed to trifluoroacetic acid-d. The peaks at 1.60–1.65 and 2.34–2.39 ppm are attributed to methylene ($-\text{CH}_2$) in AA and PA6 and those at 12.00–12.11 ppm to carboxyl ($-\text{COOH}$) in AA. The two distinct peaks at 2.79 and 2.69 ppm merge together at 2.83–2.88 ppm and are attributed to the $-\text{CH}_2$ adjacent to $-\text{NH}$ and the $-\text{NH}_2$ neighbor in DETA. The peaks at 3.66–3.71 are attributed to the $-\text{O}-\text{CH}_2-$ in RE-900 [29]. Therefore, the spectra confirmed that PA6 was successfully copolymerized without any impurity.

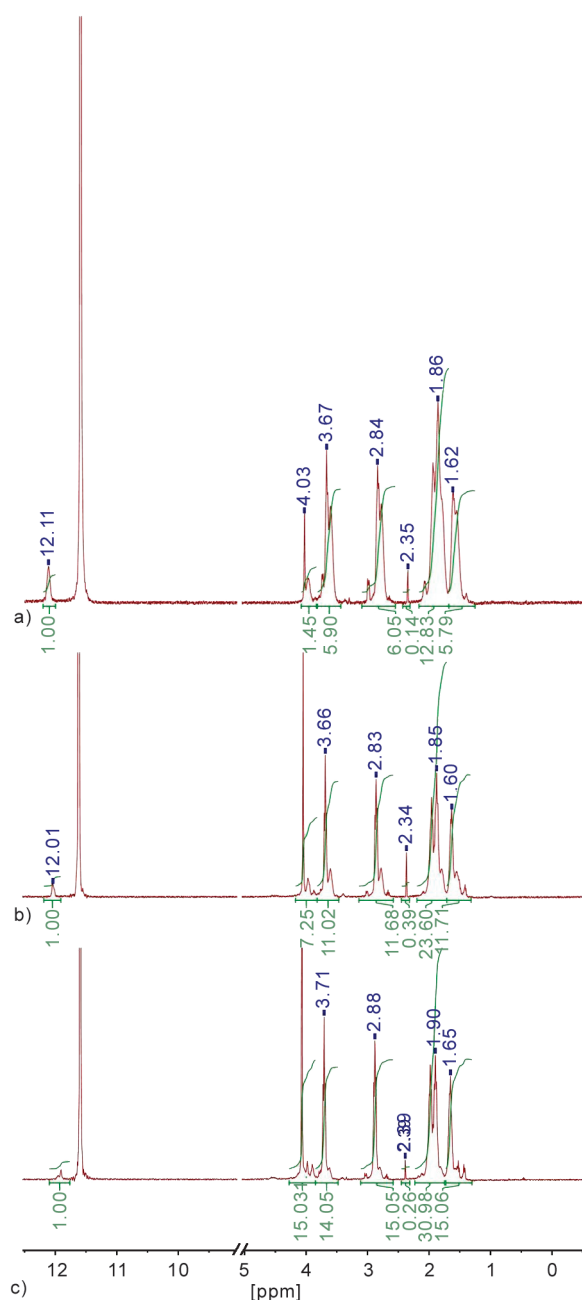


Figure 3. NMR spectra of the a) PA6-5, b) PA6-10 and c) PA6-15 copolymers.

3.2. FT-IR spectroscopy

The FT-IR spectra of the neat PA6, as well as the PA6-5, PA6-10, and PA6-15 copolymers are shown in Figure 4. The FT-IR peaks for the neat PA6 occur at the 3296.10 cm^{-1} band, attributed to the N–H bending vibration in the primary amine; two distinct bands at 2932.97 and 2862.13 cm^{-1} are attributed to asymmetric and symmetric C–H stretching of the ethylene sequence, respectively; the 1635.06 cm^{-1} band is related to C=O amide I stretching and the 1536.84 cm^{-1} band, attributed to the combined absorbance of N–H and C–N amide II stretching [30–32]. Since FT-IR spectroscopy cannot clearly determine the presence of DETA functional groups and can only confirm the presence of N–H groups, we thus focused on the content analysis of C–O ester (RE-900). An additional broadened peak can be observed at 1120.52 , 1106.82 , and 1100.21 cm^{-1} in PA6-5, PA6-10, and PA6-15, respectively, responsible for the C–O ester introduced by the use of RE-900; indeed, the area of this peak increases with the quantity of RE-900.

3.3. Relative viscosity

Table 1 indicates that the *RV*s of the copolymerized PA6-5 (1.85), PA6-10 (1.56), and PA6-15 (1.43) are significantly smaller than that of the neat PA6 (2.36). In addition, the *RV* gradually decreases with an increase in RE-900 content. This is clearly the predominant effect of amines, which have low viscosity; as the number of amide groups increases from 39 in PA6-5 to 72 in PA6-15, the *RV* drops from 1.85 to 1.43. PA6 *RV* 2.36 can meet the spinnability viscosity. The main reason for the reduction in *RV* is the

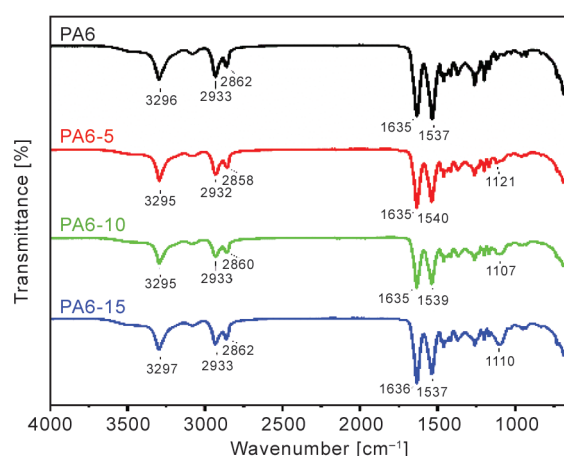


Figure 4. FT-IR spectra of PA6, PA6-5, PA6-10 and PA6-15 copolymers.

presence of copolymer RE-900, which has a higher compatibility with the test solvent (sulfuric acid) and therefore, achieves better flowability. The resulting solution was finally tested with an automated viscometer and showed a much lower relative viscosity. However, the melt spinnability of PA copolymers is not affected by solvents. Therefore, the spinnability of PA copolymer must be confirmed through thermal property analysis and actual spinning.

3.4. Thermal properties

The DSC cooling and heating curves of neat PA6, PA6-5, PA6-10, and PA6-15 are shown in Figure 5. As detailed in Table 2, the melting point and crystallization temperature of the neat PA6 are 222.3 and 173.8 °C, respectively. In contrast, the melting points of PA6-5, PA6-10, and PA6-15 are 216.3, 216.8, and 214.5 °C, respectively, and the crystallization temperatures are 173.7, 173.8, and 171.2 °C, respectively. Clearly, the addition of RE-900 decreases the melting point of a PA6 copolymer to below that of neat PA6. However, the variation of the RE-900 quantity within 15 wt% did not significantly influence the melting point, with the values for all specimens remaining close. These results agree with findings reported by Kaynak and Zolfagharian [2] that the melting point changes little with the polyetheramine content used to modify PA6. Pure PA6

exhibits double melting peaks corresponding to the α - and γ -form crystals, whereas a single peak appears in copolymers with high RE-900 contents. As polyetheramine has a soft segment structure, a small quantity does not affect the overall structural disorder (ΔS) and can stabilize crystallization. At a sufficiently high proportion (15%), the disorder (ΔS) gradually increases and the crystallinity gradually decreases as enthalpy is reduced.

3.5. Mechanical properties

The tenacity–elongation curves of the various PA6 DTYs are shown in Figure 6; the ultimate tenacities and elongations of these DTYs are shown in Table 3. The neat PA6 DTY exhibits a higher tenacity than the PA copolymer DTYs (particularly PA6-15), corresponding to a higher ultimate breaking force for the former. This may be a result of the addition of diamine, which considerably decreased the crystallinity and thereby lowered the tenacity of the PA6 copolymer fibers. Furthermore, the elongation of the PA6-15 DTY is much higher than that of the neat PA6 DTY. These results agree with those of Oh *et al.* [33], who observed a similar enhancement in elongation at break. This can be attributed to the increase in chain entanglement owing to branch formation, which increases with molecular weight. The PA6-15 DTY exhibits the lowest breaking strength of

Table 2. Thermal properties of neat PA6, PA6-5, PA6-10, and PA6-15 copolymers.

Sample	T_m [°C]	T_c [°C]	Enthalpy heating [J/g]	Crystallinity heating [%]	Enthalpy cooling [J/g]	Crystallinity cooling [%]
PA6	222.3	173.8	46.5	24.4	49.4	25.9
PA6-5	216.3	173.7	41.0	21.5	47.1	24.7
PA6-10	216.8	173.8	41.6	21.8	47.3	24.8
PA6-15	214.5	171.2	37.5	19.7	39.5	20.7

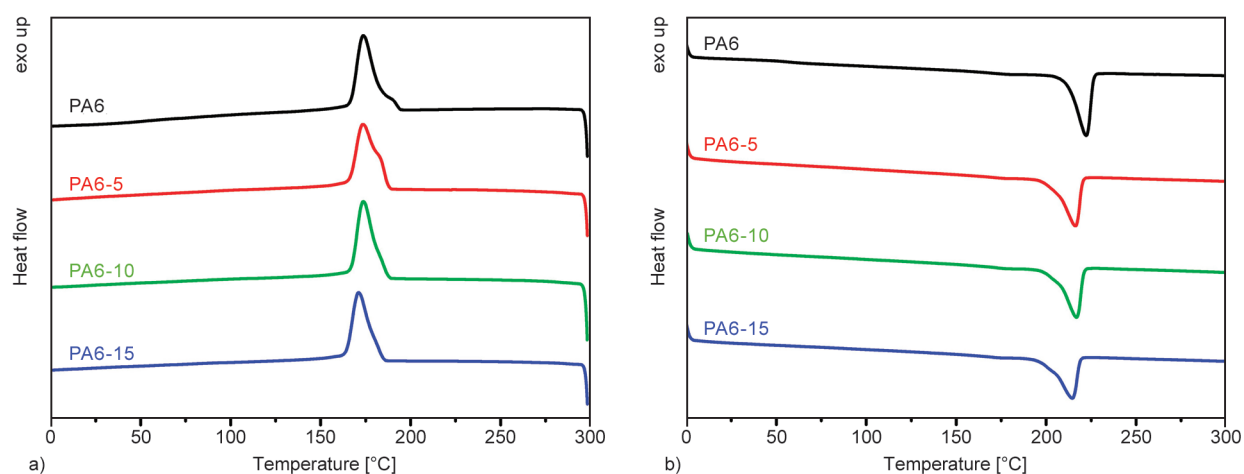


Figure 5. a) Cooling and b) heating curves of neat PA6, PA6-5, PA6-10, and PA6-15 copolymers.

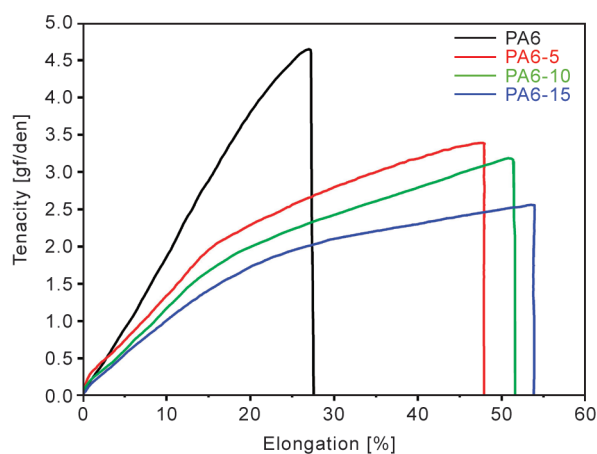


Figure 6. Tenacity–elongation curves of various PA6 DTYs.

Table 3. Mechanical properties of various PA6 DTYs with coefficients of variation (CV)

DTY	Tenacity/CV [(g/den)/%]	Elongation/CV [%/%]
PA6	4.51/2.8	26.7/3.9
PA6-5	3.36/2.3	45.8/2.4
PA6-10	3.15/1.9	50.7/2.3
PA6-15	2.53/3.4	53.9/4.1

2.53 g/den, indicating that it would be difficult to weave and process. Although the neat PA6 DTY exhibits the highest strength of 4.51 g/den, the PA6-10 DTY exhibits a breaking strength of 3.15 g/den, indicating that it could be readily woven into fabrics as well. Indeed, a higher molar ratio (>0.1) of diamines results in a higher quenching of the propagation reaction, resulting in a lower molecular weight and, consequently, reduced mechanical performance [33]. Though the modification ratio by RE-900 is less than 15%, which is insufficient to affect the polymer disorder (ΔS), enthalpy will still decrease.

Another reason for the observed decrease in DTY strength is the spinning speed. As fiber spinning is carried out at high speeds, copolymerization affects the polymer arrangement and hydrogen bond density, decreasing crystallization in the forward direction and eventually decreasing the fiber strength. However, the addition of RE-900 produces polymers with enhanced ductility, elongation, and hygroscopicity, as shown in Figure 6.

3.6. Moisture absorption and regain

The inclusion of water molecules between polymer chains causes polymers to elongate, resulting in swelling. Table 4 lists the average elongations of dif-

Table 4. Moisture absorbing elongation and dry shrinkage ratio of various PA6 DTYs.

DTY	Average moisture absorbing elongation [%]	Average dry shrinkage ratio [%]
PA6	5.9	98.1
PA6-5	8.0	96.0
PA6-10	12.0	96.1
PA6-15	15.6	94.9

ferent PA6 DTYs after moisture absorption. The average elongation of the neat PA6 DTY is 5.9%, whereas those of the PA6-5, PA6-10, and PA6-15 copolymer DTYs are 8.0, 12.0, and 15.6%, respectively. Thus, a higher quantity of diamine yields a higher percentage of hygroscopic elongation. This is a result of the high water affinity of the amine group present in diamine; Humeau *et al.* [34] made a similar observation.

Further, the average dry shrinkage ratio of the neat PA6 DTY is 98.0%; the shrinkage values for the PA6 copolymer DTYs are lower, with PA6-15 exhibiting the lowest shrinkage of 94.9%. As all PA6 copolymer DTYs exhibit high hygroscopic elongation and low dry shrinkage, a fabric made of the modified PA6 DTYs will exhibit a water-absorbing swelling-to-dry compact state interchange driven by humidity. Corresponding changes in the surface texture can be prominently observed at both the macroscopic and microscopic levels, as shown in Figure 7.

The enhanced hygroscopic elongation, together with excellent dry shrinkage, increases the porosity of the knitted fabric (as shown in Figure 7) when the humidity in the microclimate rises, reflecting the ‘pinecone effect’ and promoting the release of moisture; in contrast, the porosity decreases when the humidity level drops. The change induced by increased humidity can be observed as a transformation from a smooth to a swollen texture, as shown in the three-dimensional microscopic image of PA6-10 knitted fabric in Figure 8. Clearly, the surface of the fabric is smooth and parallel to the horizontal plane in the dry state, whereas the fabric surface swells considerably to induce a vertical variation of approximately 0.88 mm in the wet state. The Q_{\max} test was conducted on PA6-10 knitted fabric, and the heat flux value reached $0.206 \text{ W} \cdot \text{cm}^{-2}$.

Moreover, the air permeability of the PA6 copolymer fabric is higher than that of the neat PA6 fabric. This moisture-driven smart textile accordingly prevents the garment from sticking to the skin, maintaining a

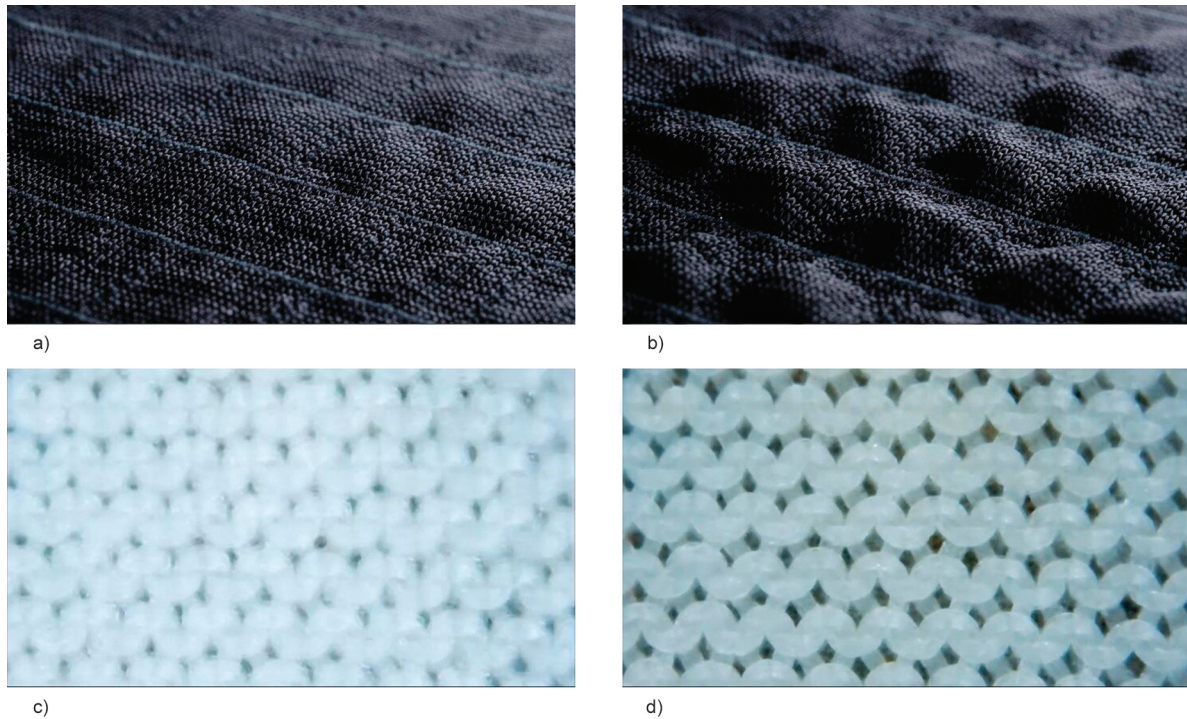


Figure 7. Variation of macroscopic surface texture in the a) dry and b) wet states and in the microscopic surface texture in the c) dry and d) wet states for PA6-10 fabric.

comfortable microclimate that is cooler and drier than that provided by ordinary textiles. During exercise, this fabric can absorb sweat from the surface of human skin and swell to regulate body heat and moisture; after exercise, the fibers sense changes in the microclimate of the human body to reduce body heat dissipation and maintain long-term comfort. Moisture-regaining tests were also performed to confirm the repeatability and durability of the observed fabric behaviors. Moisture regain was determined by conducting tests on the different fabric

Table 5. Moisture regains of various PA6 fabrics.

Sample	20 °C, 65%RH [%]	30 °C, 90%RH [%]	Moisture regains [%]
PA6	4.7	8.0	3.3
PA6-5	5.2	9.1	3.9
PA6-10	5.8	10.1	4.4
PA6-15	6.2	11.1	4.9

specimens at 20 °C and 65%RH and at 30 °C and 90%RH. The results are listed in Table 5, which shows that the moisture regain of the PA6-5 fabric (4.9%) is much higher than that of neat PA6 fabric (3.3%) and

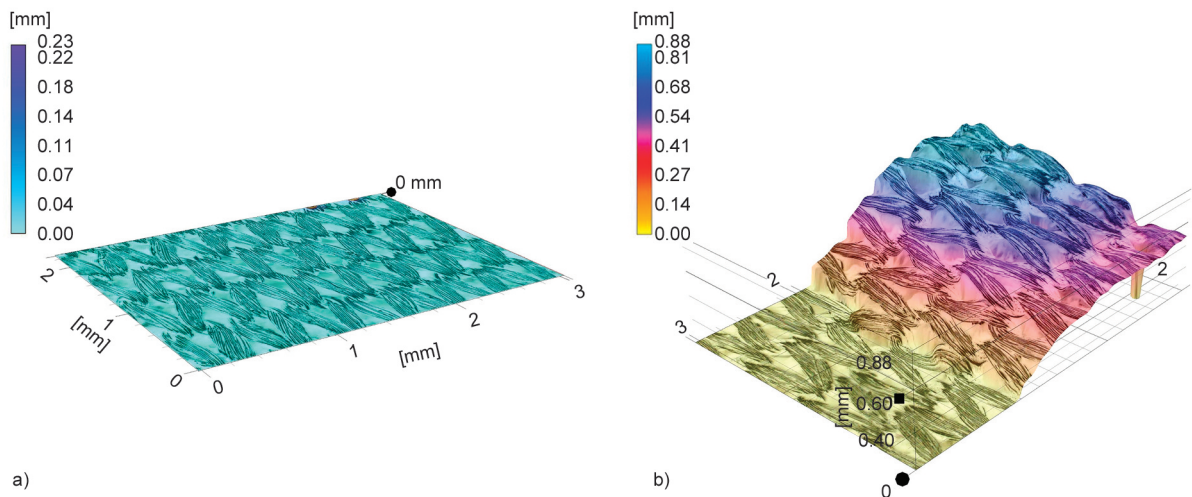


Figure 8. Swollen texture of PA6-10 copolymer fabric in the a) dry smooth and b) wet swollen state.

Table 6. Comparison of previous research on functional textiles.

Stimuli	Material	Preparation method	Product	Performance remark	References
Humidity	PET/PA6	Melt spinning	Textiles	Moisture absorption elongation 5~20%	[10]
Humidity	Proteins	Wet spinning	Silk fiber/silk muscles	Elongation during water absorption, silk muscles provided a fully reversible torsional Stroke of $547^{\circ}\cdot\text{mm}^{-1}$ when exposed to water fog.	[12]
Humidity	Graphene oxide (GO)	Coating on fabric	Textiles	Moisture management, one-way transport index R (1145%) and a desired overall moisture management capacity (0.77) within 120 s.	[13]
Heat and humidity	ZnONPs	Coating on fabric	Textiles	Heat and moisture transportation	[14]
Humidity	PA-6,6 and Jeffamine copolymer	Polymerization/melt spinning	Textiles	hydrophilicity and antibacterial activity, 10.45% of the water absorbed at 24 h/22 °C/90%RH	[22]
Thermoresponse	Poly(NIPAAm-co-HEMA-co-NMA)	Coating on fabric	Textiles	Moisture management, 7.48% moisture absorption at 20 °C	[15]
pH-triggered	Polyamines and pyromellitic diester diacid chloride copolymer	Polymerization	Microcapsules	Retain a volatile core over a long period in a dry or hydrophobic, controlled release at pH 7.4 and accelerated release at pH 5 and pH 10	[25]
Moisture-response	PA6 and polyetherdiamine copolymer	Polymerization/melt spinning	Textiles	moisture management/moisture absorption elongation 12.0% and drying recovery 96.1%/Moisture regains 4.4%	Present work

close to that of cotton fabric (approximately 4.5%). Thus, using PA6 textiles in high-moisture regions of clothing can improve touch feel and cooling performance.

A comparative study was conducted with previously reported research articles, as shown in Table 6. Research on stimulus-responsive or smart textiles has become one of the most emerging parts of academic and industrial innovation in textiles. Although the effects of many external stimuli (*e.g.*, pH) on different textile materials have been explored, researchers have mainly focused on temperature and humidity due to their rather strong effects in a wide range of applications [12–15, 25]. Various forms of products, such as silk, woven and nonwoven fabrics, polymers, microcapsules, composites, *etc.*, have been explored. However, moisture management, moisture absorbing elongation and drying recovery of PA6 fibers and fabrics have never been studied simultaneously before, which demonstrates the innovative nature of this study.

4. Conclusions

In this study, we developed a PA copolymer by copolymerizing PA6 monomer with polyetherdiamine to enhance hygroscopic elongation and

using diethylenetriamine (DETA) as a cross-linking agent. Single-component PA6 copolymeric fibers containing 5–15% polyetherdiamine were successfully melt-spun and knitted into double-layer fabrics. The resulting DTY showed significant improvements in hygroscopicity, hygroscopic elongation, dry shrinkage, and recovery compared to pure PA6. In particular, PA6-15 DTY has excellent moisture absorption elongation (15.6%) and drying shrinkage (94.9%). These results lead to the pinecone effect, in which moisture absorption causes fibers to elongate, reducing curl, and enlarging the pores in the fabric, thereby increasing breathability. Therefore, the developed hygroscopic PA fabric can prevent clothing from adhering to the skin and maintain a cool, dry, and comfortable microclimate with a Q_{max} value of $0.206 \text{ W}\cdot\text{cm}^{-2}$. PA6 copolymeric fibers utilizing the ‘environmental humidity’ mechanism, have excellent hygroscopic properties and have ‘hygroscopic elongation and drying recovery properties’, making it suitable for use in clothing to achieve high breathability of fabrics.

Acknowledgements

The work was supported by the Ministry of Science and Technology of Taiwan, ROC under contract number MOST 110-2221-E-011-006-MY3.

References

- [1] Hu J., Meng H., Li G., Ibekwe S. I.: A review of stimuli-responsive polymers for smart textile applications. *Smart Materials and Structures*, **21**, 053001 (2012). <https://doi.org/10.1088/0964-1726/21/5/053001>
- [2] Kaynak A., Zolfagharian A.: Stimuli-responsive polymer systems – Recent manufacturing techniques and applications. *Materials*, **12**, 2380 (2019). <https://doi.org/10.3390/ma12152380>
- [3] Ruckdashel R. R., Venkataraman D., Park J. H.: Smart textiles: A toolkit to fashion the future. *Journal of Applied Physics*, **129**, 130903 (2021). <https://doi.org/10.1063/5.0024006>
- [4] Zhang Q., Rudolph T., Benitez A. J., Gould O. E., Behl M., Kratz K., Lendlein A.: Temperature-controlled reversible pore size change of electrospun fibrous shape-memory polymer actuator based meshes. *Smart Materials and Structures*, **28**, 055037 (2019). <https://doi.org/10.1088/1361-665X/ab10a1>
- [5] Yin Z., Shi S., Liang X., Zhang M., Zheng Q., Zhang Y.: Sweat-driven silk-yarn switches enabled by highly aligned gaps for air-conditioning textiles. *Advanced Fiber Materials*, **1**, 197–204 (2019). <https://doi.org/10.1007/s42765-019-00021-y>
- [6] Gernhardt M., Peng L., Burgard M., Jiang S., Förster B., Schmalz H., Agarwal S.: Tailoring the morphology of responsive bioinspired bicomponent fibers. *Macromolecular Materials and Engineering*, **303**, 1700248 (2018). <https://doi.org/10.1002/mame.201700248>
- [7] Liu X., Li Y., Hu J., Jiao J., Li J.: Smart moisture management and thermoregulation properties of stimuli-responsive cotton modified with polymer brushes. *RSC Advances*, **4**, 63691–63695 (2014). <https://doi.org/10.1039/C4RA11080C>
- [8] Chung C., Mi L., Kuan S. L., Chen Y. I., Wang C. P.: Adjustable-transition-temperature flexible temperature-sensitive polymer material for textiles. CN105859957A, China (2016).
- [9] Height M., Sieber H.: Functional thermo-regulating textile additives and uses thereof. WO2019086322, U.S. (2019).
- [10] Yoshimoto M., Yasui S., Morioka S., Nakajima S.: Conjugate fiber-containing yarn. CN101395307B, China (2012).
- [11] Yasui S., Yamaguchi T., Yoshimoto M., Morioka S.: Woven/knit fabric including crimped fiber and becoming rugged upon humidification, process for producing the same, and textile product. WO2006041200A1, China (2006).
- [12] Jia T., Wang Y., Dou Y., Li Y., de Andrade M. J., Wang R., Fang S., Li J., Yu Z., Qiao R., Liu Z., Cheng Y., Su Y., Jolandan M. M., Baughman R. H., Qian D., Liu Z.: Moisture sensitive smart yarns and textiles from self-balanced silk fiber muscles. *Advanced Functional Materials*, **29**, 1808241 (2019). <https://doi.org/10.1002/adfm.201808241>
- [13] Guan X., Wang X., Huang Y., Zhao L., Sun X., Owens H., Lu J. R., Liu X.: Smart textiles with Janus wetting and wicking properties fabricated by graphene oxide coatings. *Advanced Materials Interfaces*, **8**, 2001427 (2021). <https://doi.org/10.1002/admi.202001427>
- [14] Noman M. T., Petru M., Louda P., Kejzlar P.: Woven textiles coated with zinc oxide nanoparticles and their thermophysiological comfort properties. *Journal of Natural Fibers*, **19**, 4718–4730 (2022). <https://doi.org/10.1080/15440478.2020.1870621>
- [15] Chaudhuri S., Wu C-M.: Switchable wettability of poly(NIPAAm-co-HEMA-co-NMA) coated PET fabric for moisture management. *Polymers*, **12**, 100 (2020). <https://doi.org/10.3390/polym12010100>
- [16] Zhang S., Zhang J., Tang L., Huang J., Fang Y., Ji P., Wang C., Wang H.: A novel synthetic strategy for preparing polyamide 6 (PA6)-based polymer with transesterification. *Polymers*, **11**, 978 (2019). <https://doi.org/10.3390/polym11060978>
- [17] Cousin T., Galy J., Rousseau A., Dupuy J.: Synthesis and properties of polyamides from 2,5-furandicarboxylic acid. *Journal of Applied Polymer Science*, **135**, 45901 (2018). <https://doi.org/10.1002/app.45901>
- [18] Bakkali-Hassani C., Planes M., Roos K., Wirotius A-L., Ibarboure E., Carlotti S.: Synthesis of polyamide 6 with aramid units by combination of anionic ring-opening and condensation reactions. *European Polymer Journal*, **102**, 231–237 (2018). <https://doi.org/10.1016/j.eurpolymj.2018.03.027>
- [19] Peng S., Peng L., Yi C., Zhang W., Wang X.: A novel synthetic strategy for preparing semi-aromatic components modified polyamide 6 polymer. *Journal of Polymer Science A*, **56**, 959–967 (2018). <https://doi.org/10.1002/pola.28983>
- [20] Dutkiewicz S., Boryniec S.: Synthesis and characteristics of modified polyamides based on lactams and polyetheramines. *Polimery*, **48**, 116–121 (2003). <https://doi.org/10.1177/0307174X0303000619>
- [21] Dike A. S.: Improvement of mechanical and physical properties of carbon fiber-reinforced polyamide composites by applying different surface coatings for short carbon fiber. *Journal of Thermoplastic Composite Materials*, **33**, 541–553 (2019). <https://doi.org/10.1177/0892705719877218>
- [22] Rossi F., Zaltieri M., Sacchetti A., Masi M.: Functionalization of nylon-6,6 with polyetheramine improves wettability and antibacterial properties. *Industrial and Engineering Chemistry Research*, **60**, 10666–10673 (2021). <https://doi.org/10.1021/acs.iecr.1c00427>
- [23] Okabe T., Takehara T., Inose K., Hirano N., Nishikawa M., Uehara T.: Curing reaction of epoxy resin composed of mixed base resin and curing agent: Experiments and molecular simulation. *Polymer*, **54**, 4660–4668 (2013). <https://doi.org/10.1016/j.polymer.2013.06.026>

- [24] Ferdosian F., Yuan Z., Anderson M., Xu C.: Sustainable lignin-based epoxy resins cured with aromatic and aliphatic amine curing agents: Curing kinetics and thermal properties. *Thermochimica Acta*, **618**, 48–55 (2015). <https://doi.org/10.1016/j.tca.2015.09.012>
- [25] Wang H-C., Grolman J. M., Rizvi A., Hisao G. S., Rienstra C. M., Zimmerman S. C.: pH-triggered release from polyamide microcapsules prepared by interfacial polymerization of a simple diester monomer. *ACS Macro Letters*, **6**, 321–325 (2017). <https://doi.org/10.1021/acsmacrolett.6b00968>
- [26] Gissinger J. R., Jensen B. D., Wise K. E.: Modeling chemical reactions in classical molecular dynamics simulations. *Polymer*, **128**, 211–217 (2017). <https://doi.org/10.1016/j.polymer.2017.09.038>
- [27] Boonying P., Martwiset S., Amnuaypanich S.: Highly catalytic activity of nickel nanoparticles generated in poly(methylmethacrylate)@poly(2-hydroxyethylmethacrylate) (PMMA@PHEMA) core-shell micelles for the reduction of 4-nitrophenol (4-NP). *Applied Nanoscience*, **8**, 475–488 (2018). <https://doi.org/10.1007/s13204-018-0669-0>
- [28] Winnacker M.: Polyamides and their functionalization: Recent concepts for their applications as biomaterials. *Biomaterials Science*, **5**, 1230–1235 (2017). <https://doi.org/10.1039/C7BM00160F>
- [29] García M., van Vliet G., ten Cate M. G. J., Chávez F., Norder B., Kooi B., van Zyl W. E., Verweij H., Blank D. H. A.: Large-scale extrusion processing and characterization of hybrid nylon-6/SiO₂ nanocomposites. *Polymers for Advanced Technologies*, **15**, 164–172 (2004). <https://doi.org/10.1002/pat.458>
- [30] Aguilar J. C. F., Moreno M. J. R., Jurado L. T., Ramirez H. B.: Low pressure and low temperature synthesis of polyamide-6 (PA6) using Na⁰ as catalyst. *Materials Letters*, **136**, 388–392 (2014). <https://doi.org/10.1016/j.matlet.2014.08.071>
- [31] Tang J., He N., Nie L., Xiao P., Chen H.: Hydrolysis of microporous polyamide-6 membranes as substrate for in situ synthesis of oligonucleotides. *Surface Science*, **550**, 26–34 (2004). <https://doi.org/10.1016/j.susc.2003.12.020>
- [32] Kherroub D. E., Belbachir M., Lamouri S., Larbi B., Chikh K.: Synthesis of polyamide-6/montmorillonite nanocomposites by direct *in-situ* polymerization catalysed by exchanged clay. *Oriental Journal of Chemistry*, **29**, 1429–1436 (2014). <https://doi.org/10.13005/ojc/290419>
- [33] Oh K., Kim H., Seo Y.: Effect of diamine addition on structural features and physical properties of polyamide 6 synthesized by anionic ring-opening polymerization of ε-caprolactam. *ACS Omega*, **4**, 17117–17124 (2019). <https://doi.org/10.1021/acsomega.9b01342>
- [34] Humeau C., Davies P., LeGac P-Y., Jacquemin F.: Influence of water on the short and long term mechanical behaviour of polyamide 6 (nylon) fibres and yarns. *Multiscale Multidisciplinary Modeling, Experiments and Design*, **7**, 317–327 (2018). <https://doi.org/10.1007/s41939-018-0036-6>